[redacted]

NASA TECHNICAL MEMORANDUM

NASA TM X-52023

29p.

N64-20576

CODE-1

NASA TM X-52023

RADIATION PROCESSES RELATED TO OXYGEN-HYDROGEN COMBUSTION AT HIGH PRESSURES

by Marshall C. Burrows
Lewis Research Center
Cleveland, Ohio

TECHNICAL PREPRINT for Tenth International Symposium on Combustion sponsored by the Combustion Institute and the Cambridge Physical Chemistry Department
Cambridge, England, August 17-21, 1964

OTS PRICE

XEROX $ [redacted]

NATIONAL AERONAUTICS AND SPACE ADMINISTRATION · WASHINGTON, D.C. · 1964

TECHNICAL MEMORANDUM

RADIATION PROCESSES RELATED TO OXYGEN-HYDROGEN COMBUSTION AT HIGH PRESSURES

by Marshall C. Burrows
Lewis Research Center
Cleveland, Ohio

TECHNICAL PREPRINT prepared for

Tenth International Symposium on Combustion
sponsored by the Combustion Institute and the
Cambridge Physical Chemistry Department
Cambridge, England, August 17-21, 1964

NATIONAL AERONAUTICS AND SPACE ADMINISTRATION

RADIATION PROCESSES RELATED TO OXYGEN-HYDROGEN COMBUSTION AT HIGH PRESSURES

by Marshall C. Burrows
National Aeronautics and Space Administration
Lewis Research Center
Cleveland, Ohio

E-2566

SUMMARY

Radiation related to the combustion of liquid-oxygen jets in a gaseous hydrogen atmosphere was studied by measuring the intensities of OH, O_2, and H_2O radiation in a combustion chamber equipped with windows. Overall oxidant-fuel weight ratio was varied from 1 to 10 at a chamber pressure of 24 atmospheres. Maximum intensities from the radiating species were obtained near stoichiometric mixture ratios. Gas temperatures derived from the measured color temperature of a tungsten plate in the gas stream agreed with theoretical temperatures of the products. Gas radiation appeared to be thermally excited and in local equilibrium at all locations within the combustor.

Radiation measurements made in the upstream region of a stable combustor showed that intensities varied little with oxidant-fuel weight ratio. Measured intensities initially increased in the direction of gas flow due to the increased extent of reaction and then decreased when diluted with excess reactant or cooled by heat transfer to the walls. Ultraviolet and total radiation data showed that the reaction proceeded at approximately a constant rate until

the limiting reactant was consumed. The distance required to complete the reaction varied from 1.5 to 12 inches for a variation in oxidant-fuel weight ratio of 1 to 9.

During combustion with pressure and velocity oscillations along the axis of the combustion chamber, average intensities of the radiating gases showed that the axial distance required to react the liquid oxygen and hydrogen was reduced. The distance required to complete the reaction in this case varied from 1 to 6 inches for an oxidant-fuel weight-ratio variation of 1 to 9.

The extent of reaction as determined by radiation measurements in the two combustors was compared to the predicted trends where turbulent mixing or vaporization were considered to control the reaction.

INTRODUCTION

Various analytical models of the combustion processes in liquids and gases have considered the role of vaporization rate[1], turbulent mixing rate[2], and chemical reaction rate[3] in efforts to determine the rate-controlling processes of various reactants. An experimental method of measuring these rates would be a valuable tool for the analysis of stable and unstable combustion processes.

In this paper, the overall processes controlling the combustion of liquid oxygen and gaseous hydrogen were related to radiation from several molecular species along the axis of a high-pressure combustor. Previous work has established the thermal

origin of the radiation[4,5,6] and therefore makes it possible to relate radiation intensities to the reaction process and equilibrium products and heat losses to the combustor walls. Data are presented for stable combustion at constant pressure, and unstable combustion with a maximum pressure oscillation of 30 percent. Thermal and chemical equilibrium in the gases are discussed, and extents of reaction in the two combustors as measured by radiation intensities are compared to the calculated trends for several combustion models.

EXPERIMENTAL

A copper combustor was constructed in sections to permit the location of a section with windows at various axial distances from the injector (Fig. 1). High-velocity nitrogen parallel to the inner surfaces of the windows prevented condensation and kept the optical path free of absorbing gases. Stable combustion was provided by nine 0.032-inch liquid-oxygen jets injected axially with low-velocity hydrogen gas, hereafter referred to as combustor A. Consistently unstable combustion was provided by 45 high-velocity gaseous-hydrogen jets surrounded by liquid oxygen in 0.005-inch annuli, hereafter referred to as combustor B. Both combustors were operated over a range of oxygen and hydrogen flows to obtain oxidant-fuel weight-ratio variations (o/f) from 1 to 10±0.1. Calculated oxygen velocities varied from 60 to 100 feet per second in combustor A and from 35 to 60 feet per second in combustor B. Data are presented for an average chamber pressure of 24 atmospheres.

Emission spectra from the combustor window were recorded photographically in the ultraviolet and visible spectral region on a 1.5-meter grating spectrograph. With a spectral slitwidth of 1.109 Angstroms (Å), exposures of 3 seconds were sufficient to expose type 1-0 Kodak film. Infrared spectra were obtained by a monochromator equipped with a calcium fluoride prism and indium antimonide detector. Spectral slitwidth was approximately 1000 Å. The spectral region from 6000 to 35000 Å was scanned in approximately 6 seconds, and detector outputs were recorded as a function of wavelength.

Ultraviolet radiation passed through a 0.50-inch restriction and quartz window to a photometer equipped with an ultraviolet filter (Corning 7-54) in front of a photomultipler (RCA 1 P 28). Spectral response of the unit extended from 2400 to 4000 Å with a broad maximum at 3000 to 3200 Å. The photomultiplier was operated within its linear range, and its output was monitored by a X-Y plotter from which average intensities were measured during each run. Precision of the measurements was approximately ±10 percent. Runs were duplicated at least once to insure reproducibility of data.

Total radiation was transmitted through the 1-inch window port to a pyrometer with parabolic mirrors focusing the radiation on a thermocouple. Spectral response of the pyrometer was limited by the quartz combustor windows to 2000 to 35000 Å. Run duration was at least 5 seconds to allow the pyrometer sufficient time to respond to the radiation. Maximum pyrometer readings during each run

were reproducible within ±10 percent.

Output voltages from the pyrometer were directly proportional to the total radiation intensities. Calibration with a tungsten lamp showed that the voltage e varied according to the relation $e = \alpha T^{4.33}$ where α is a calibration constant equal to 4.48×10^{-18} volts per ^{o}K and T is the color temperature in ^{o}K.

RESULTS

Spectra

Spectra of the gases within the combustor (Fig. 2) show that predominant radiation in the ultraviolet and visible spectral region is due to the hydroxyl radical (OH) with the maximum intensities concentrated around 3100 Å. Weaker spectral lines between 3200 and 4500 Å are largely due to molecular oxygen radiation (Schumann-Runge bands). The infrared spectra show the characteristic water-vapor bands centered near 14000, 19000, and 27000 Å. The OH radical also has emission bands near these wavelengths, but they are masked by the stronger H_2O bands and therefore cannot be distinguished.

Ultraviolet Radiation

A photometer was used to measure the ultraviolet radiation emitted by the gases in the combustor. Average ultraviolet radiation intensities were measured as a function of axial distance from the injector in combustors A and B (Fig. 3). Overall oxidant-fuel weight ratios were varied from 1 to 9 in combustor A and from 3 to 10.5 in combustor B. Radiation near the injector in combustor A

increased at approximately a constant rate with axial distance. Maximum ultraviolet radiation intensities occurred approximately 1.5 inches from the injector at an o/f of 1 and 8-inches downstream at an o/f of 7. Data were not obtained from combustor A at axial distances greater than 13 inches from the injector. Radiation thereafter was extrapolated as a straight dashed line for each o/f. Apparent decreases in radiation after the maxima occurred at rates which varied from 1.4 to 2.8 percent per inch of combustor length.

Combustor B was operated at the same average pressure as combustor A, but with a high-frequency pressure oscillation with peak-to-peak amplitudes that varied from 5 to 30 percent of the average pressure. Intensities measured by the photometer showed that radiation increased at very high rates near the injector of combustor B with the rate increasing with overall mixture ratio to a maximum at an o/f of 9. Maximum ultraviolet intensities occurred at approximately one-half the distance from the injector as compared to stable combustion (Figs. 3(a) and (b)). The decrease in radiation intensities thereafter was larger during unstable combustion, with a rate which varied from 3.5 to 4.5 percent per inch of combustor length.

Total Radiation

A total radiation pyrometer was used to measure the total radiance from the gases within the chamber. Total radiation intensities varied with axial distance from the injector as shown in

Fig. 4 for combustors A and B.

Total radiation near the injector of combustor A increased at approximately a constant rate with distance, similar to the behavior of the ultraviolet radiation. Maximum total radiation occurred approximately at 1.5 inches from the injector for an o/f of 0.8, 6 inches for an o/f of 4.9, and 12 inches for an o/f of 9. The radiation at distances greater than 13 inches appeared to be constant and was extrapolated as a dashed line.

Total radiation intensities in combustor B increased at very high rates near the injector. Maximum total radiation occurred at approximately 0.8 inch from the injector for an o/f of 1 and increased to 6 inches for an o/f of 7.5. At downstream distances greater than 12 inches, measured radiation intensities remained nearly constant.

Gas Temperature

Gas temperatures were experimentally derived as a function of the overall mixture ratio 12 inches from the injector in combustor A. An oxidized tungsten plate with a high surface emittance[7] was placed in the center of the combustor, and the pyrometer was focused on its surface through the combustor window. Total radiation from the plate is shown as curve A in Fig. 5 as a function of o/f. When the equation relating the pyrometer voltage to temperature is used and the emittance of the tungsten is assumed to be one, the radiation data show that the apparent plate temperature increases from $1200 \pm 50^{\circ}$ K at an o/f of 1 to $3240 \pm 100^{\circ}$ K at an

o/f of 9. These temperatures are somewhat lower than the calculated temperatures for equilibrium gas mixtures[8,9,10] that varied from 1250° K at an o/f of 1 to a maximum of 3470° K at an o/f of 8. Plate radiation, corrected for plate emittance, window absorption, and heat-transfer losses, would give plate temperatures quite close to calculated temperatures for equilibrium gas mixtures. The average temperature of the gases heating the tungsten plate was therefore substantially that of the calculated temperature, indicating that the reaction was complete 12 inches from the injector. The total gas radiation at 12 inches from the injector is plotted as curves B and C in Fig. 5 for combustors A and B, respectively. Intensities are lower than those for the tungsten plate.

DISCUSSION

Thermal Equilibrium

The spectrograms of emitted radiation from combustors A and B indicated that the principal ultraviolet emission was from the OH radical and that infrared radiation was primarily from H_2O. It was assumed that the ultraviolet photometer measured average intensities of the OH radical emission centered at 3100 Å and that the total radiation pyrometer measured average intensities of the H_2O emission centered at 24000 Å.

A decrease in ultraviolet radiation intensities was shown at large axial distances from the injector in Fig. 3. Since previous work has shown that the OH radical is thermally excited in the combustor[4,5], the decrease in radiation intensities was assumed to be due to the decreasing temperature of the gases caused by heat

transfer to the chamber walls. Heat-transfer rates to the walls can be estimated from the calculated temperature decrease and the reduced enthalpy of the gases. The decrease in gas temperature corresponding to a decrease in the radiation intensity was calculated from Planck's radiation law. A wavelength of 3100 Å, initial gas temperature of 3470° K, and constant gas emissivity were assumed. An average radiation decrease in combustor A of 2.0 percent per inch results in a temperature decrease of 60° K in 10 inches. The corresponding decrease in the enthalpy of the gases results in a calculated heat-transfer rate of 4 Btu per square inch per second to the walls. This value is close to the measured rate of 4 to 5 Btu per square inch per second in a similar combustor[11]. Ultraviolet radiation in combustor B decreased at approximately twice the rate measured in combustor A, indicating higher heat transfer to the walls during unstable combustion.

In a well-mixed adiabatic system, thermally excited ultraviolet intensities would rise to limiting values for each o/f and thereafter remain constant with increasing axial distance. If the limiting value of radiation is assumed to be reached when the reaction is completed, the maximum intensities in the two combustors indicate the approximate end of reaction. The axial distance required to complete the reaction in combustor A (Fig. 3) varied from 1.5 to 8 inches for a variation in oxidant-fuel weight ratio from 1 to 9. By contrast, the reaction was completed in approximately one-half this distance during unstable combustion with combustor B.

Infrared radiation is much less sensitive to a small temperature change in the gases, so heat-transfer effects on these radiation intensities are small. For example, it was previously shown that a 20-percent decrease in ultraviolet radiation at 3100 Å could be caused by only a 60° K decrease in temperature. This same temperature decrease would decrease H_2O radiation at 24000 Å by only 3.3 percent. This effect is shown in Fig. 4(b) where the total radiation intensities at distances larger than 12 inches from the injector are nearly constant. The small variations that do occur at low o/f's are probably due to a lower overall mixing with large quantities of excess hydrogen. For the infrared data, it was again assumed that the reaction was completed at maximum total intensities. In combustor A, the distance required for complete reaction varied from 1.5 to 12 inches for an o/f variation from 1 to 9. In combustor B, this distance was reduced to 0.8 to 6 inches. The agreement between the total (H_2O) and ultraviolet (OH) radiation data indicates probable thermal equilibrium in the combustors.

Chemical Equilibrium

The previously indicated close agreement between the plate temperatures and equilibrium gas temperatures in combustor A indicates probable chemical equilibrium of the products. A further check on both chemical and thermal equilibrium of the products can be made by comparing the observed radiation to calculated radiation based on chemical equilibrium temperatures and concentrations.

Calculated OH intensities at 3100 Å vary with o/f according to the relation[12]

$$I_{\Delta\lambda} = \left(1 - e^{-K_{\Delta\lambda} P_{OH}^{L} T_o/T}\right) \frac{C_1}{\lambda^5 \left(e^{C_2/\lambda T} - 1\right)}$$

where

$I_{\Delta\lambda}$ band intensity of OH

$K_{\Delta\lambda}$ integrated absorption coefficient of OH band, assumed equal to 0.89 cm^{-1} atm^{-1} from Ref. 12

P_{OH} equilibrium concentration of OH in atmospheres[8,9,10]

L path length of 5 cm

T_o/T correction for temperatures different from T_o equal to 2877° K

C_1, C_2 constants in Planck's radiation law

λ effective wavelength of 3100 Å

T equilibrium gas temperature

Calculated OH concentrations, temperatures, emissivities, and intensities are tabulated in Table I for mixture ratios between 1 and 10. These calculated intensities vary with o/f as shown in curve B in Fig. 6. If the OH emissivity is unity (exponent containing $K_{\Delta\lambda}$ is very large) at all mixture ratios, radiation intensities vary only with the temperature at each o/f as shown by curve A in Fig. 6. It is expected that OH in thermal and chemical equilibrium within the combustors will vary with o/f in a manner similar to the calculated trends. Measured ultraviolet intensities 12 inches from the injector in combustors A

and B were corrected for the heat-transfer losses mentioned previously and plotted as curves (c) and (d), respectively, in Fig. 6. The shapes of the calculated curves compare favorably with that of combustor B. Combustor A radiation does not conform to the trends in calculated intensities, especially in that intensities were much higher than those calculated at the lower o/f ratios. Since the average gas temperatures in this combustor were close to the calculated equilibrium temperatures, the observed variation must be due to insufficient uniformity in the gases. High temperature zones at low overall mixture ratios will increase the average OH intensities to abnormal values. This can be illustrated by averaging the intensities obtained from a sinusoidal variation in o/f. Varying the local o/f 20 percent above and below a value of 4 (3.2 to 4.8) increases the average OH intensity 1.95 times that for a gas at an o/f of 4.

The lack of homogeneous gases in the stable combustor A appears to be due to the lack of adequate mixing. In combustor B mixing is accomplished by the high velocities associated with the axial pressure oscillation.

Intensity of water-vapor emission in the infrared region depends on the integrated intensities of bands at 11000, 14000, 19000, and 27000 Å.[12] When the total radiation data at 12 inches from the injector in combustors A and B are compared to the radiation intensities of the tungsten plate, total emissivities of the gases are considerably below that of the plate (Fig. 5). If the

gases are at the calculated temperature of equilibrium products, the apparent emissivity of the gases in combustor A varied from 0.15 to 0.075. Apparent emissivities of combustor B products varied from 0.7 to 0.25.

The data that are available on water-vapor radiation[12] indicate that gas emissivities in the combustors should be less than 0.15. Combustor B gases therefore emit higher than expected intensities. Radiation from the chamber wall and quartz window may have contributed to at least part of the high radiation observed. An additional difference between the measured plate radiation and gas radiation can be due to a slight change in the solid angle observed by the pyrometer. The temperature effect on radiation intensities is much lower in the infrared region, and the H_2O concentration increases with o/f much slower than OH concentration. The anomalous behavior of OH radiation in combustor A (Fig. 6) does not appear in the infrared data in Fig. 5.

Because the radiation for well mixed and uniform products 12-inches downstream varied according to theoretical calculations, it is concluded that the gases were in chemical equilibrium.

Extent of Reaction

The processes which make up the mechanisms of oxygen vaporization, mixing, reaction, and establishment of equilibrium products can be outlined on the basis of the preceding data. During stable combustion, OH and H_2O intensities near the injector are nearly independent of the overall oxidant-fuel weight ratio. Temperatures near the injector are also independent of the overall mixture

ratio.[5] It is believed, therefore, that the reaction takes place in mantles around the liquid-oxygen jets at temperatures which approach those of a stoichiometric mixture. Optical depth of the radiating gases increases directly with increased reaction, and hence the radiation intensity increases in direct proportion to the extent of reaction. After the reaction is complete (all of the O_2 or H_2 reacted), the excess reactant mixes with the products to form a homogeneous mixture that approaches the calculated equilibrium composition, temperature, and radiation intensity. During unstable combustion, the previous processes occur in the same order but within a much shorter distance in the combustor.

Turbulent mixing[2,13,14] and vaporization[1] of the reactants have both been considered to have considerable influence on the extent of reaction in a combustor. The turbulent mixing model assumes that diffusion of one reactant into the other is limited by the local turbulence intensity and the distance between injection elements. The vaporization model considers reactant vaporization (oxygen in the present case) to control the extent of reaction.

The two models were used to predict the behavior of H_2O radiation at 24000 Å in combustors A and B as a function of axial distance as shown in Fig. 7. The techniques of calculating extent of reaction by turbulent mixing are given in Refs. 2, 13, and 14; vaporization calculations are given in Ref. 1. The combustor was arbitrarily divided into three zones which included

(1) stoichiometric reaction, (2) mixing with excess hydrogen, and (3) uniform products. Radiation intensities in zone (1) varied with the concentration of H_2O in proportion to the extent of reaction. This zone was controlled by turbulent mixing or vaporization and is shown as a solid line. Radiation in zone (3) was proportional to the H_2O concentration at the temperature of equilibrium products[8,9,10], while the mixing behavior of zone (2) radiation was assumed. The latter zones are not important to this discussion and are shown as dotted and dashed lines, respectively.

Combustor parameters that influenced the turbulent mixing model were primarily the injector element spacing and the local turbulence intensity. These parameters differed by at least 20 times between combustors A and B, causing the reaction by turbulent mixing to be completed in less than 1 inch in combustor B (Fig. 7(c)).

The vaporization of liquid oxygen was controlled largely by the median drop size of oxygen produced by the injector[1]. Hence, the reaction at a mixture ratio of 8 was completed in 22 inches in combustor A (Fig. 7(b)) and in 6 inches in combustor B (Fig. 7(d)).

When the trends indicated by the calculated radiation in Fig. 7 are compared to the total measured intensities in Fig. 4, it appears that the extent of reaction is controlled by turbulent mixing in combustor A, and vaporization limits the reaction in combustor B. While refinements are desirable in the assumptions

made in these calculations, the indicated trends show the merit of comparing radiation measurements with these or similar analytical models for determining the extent of reaction for various reactants and combustor configurations.

In conclusion, agreement between the experimental and calculated ultraviolet and infrared radiation data shows that the OH and H_2O radiation within the combustor is in local thermal and chemical equilibrium. Intensities in both spectral regions can be used to determine the required distance to react liquid oxygen with hydrogen. Difficulties in determining ultraviolet intensities can be attributed to heat losses and inadequate homogeneity of the products within the combustor. Rate processes related to the combustion of liquid oxygen and hydrogen, based on a constant temperature reaction with subsequent mixing of the products, are inferred from the data and compared to calculated radiation controlled by turbulent mixing or vaporization. The reaction in the stable combustor appeared to be controlled by turbulent mixing. Vaporization apparently limited the reaction in the unstable combustor.

REFERENCES

1. Priem, Richard J., and Heidmann, Marcus A.: Propellant Vaporization as a Design Criterion for Rocket-Engine Combustion Chambers. NASA TR R-67, 1960.

2. Bittker, David A.: An Analytical Study of Turbulent and Molecular Mixing in Rocket Combustion. NACA TN 4321, 1958.

3. Bittker, David A., and Brokaw, Richard S.: Estimate of Chemical Space Heating Rates in Gas-Phase Combustion with Application to Rocket Propellants. ARS. Jour., vol. 30, no. 2, Feb. 1960, pp 179-185.

4. Burrows, Marshall C., and Provinelli, Louis A.: Emission Spectra from High-Pressure Hydrogen-Oxygen Combustion. NASA TN D-1305, 1962.

5. Burrows, Marshall C., and Razner, Ronald: Relation of Emitted Ultraviolet Radiation to the Combustion of Hydrogen and Oxygen at High Pressure. Proposed NASA TN.

6. Gaydon, A. G.: The Spectroscopy of Flames. John Wiley & Sons, Inc., 1957.

7. Pears, C. D.: Some Problems in Emittance Measurements at the Higher Temperatures and Surface Characterization. Measurement of Thermal Radiation Properties of Solids. NASA SP-31, 1963.

8. Zeleznik, Frank J., and Gordon, Sanford: A General IBM 704 or 7090 Computer Program for Computation of Chemical Equilibrium Compositions, Rocket Performance, and Chapman-Jouguet Detonations. NASA TN D-1454, 1962.

9. Gordon, Sanford, and Zeleznik, Frank J.: A General IBM 704 or 7090 Computer Program for Computation of Chemical Equilibrium Compositions, Rocket Performance, and Chapman-Jouguet Detonations. Supplement 1 - Assigned Area-Ratio Performance. NASA TN D-1737, 1963.

10. McBride, Bonnie J., Heimel, Sheldon, Ehlers, Janet G., and Gordon, Sanford: Thermodynamic Properties to 6000° K from 210 Substances Involving the First 18 Elements. NASA SP-3001, 1963.

11. Heidmann, Marcus F., and Baker, Louis, Jr.: Combustor Performance with Various Hydrogen-Oxygen Injection Methods in a 200-Pound-Thrust Rocket Engine. NACA RM E58E21, 1958.

12. Penner, S. S.: Quantitative Molecular Spectroscopy and Gas Emissivities. Addison-Wesley Pub. Co., Inc., 1959.

13. Hersch, Martin: Effect of Interchanging Propellants on Rocket Combustor Performance with Coaxial Injection. NASA TN D-2169, 1964.

14. Hersch, Martin: Private communication.

TABLE I. - CALCULATED RADIATION TERMS AS FUNCTION OF OXIDANT-FUEL WEIGHT RATIO

[$K_{\Delta\lambda}$, 0.89 cm^{-1} atm^{-1}; T_o, 2877° K; L, 5 cm]

Oxidant-fuel weight ratio, o/f	Equilibruim OH concentration, P_{OH} atm	Equilibruim gas temperature, T, °K	$K_{\Delta\lambda} P_{OH} L \frac{T_o}{T}$	Emissivity, of OH band, $\epsilon_{\Delta\lambda}$	Relative blackbody radiance, $I_{\Delta\lambda}$	$\epsilon_{\Delta\lambda} I_{\Delta\lambda}$
1	------	1260	-----	------	------	-----
2	0.0002	2015	0.001	0.001	0.05	-----
3	.022	2630	.11	.11	.9	0.01
4	.104	3030	.44	.36	9.3	3.3
6	1.176	3410	4.41	.988	51.1	51.0
8	2.116	3470	7.80	.9996	64.6	64.6
10	2.382	3420	8.94	.9999	53.1	53.1

E-2566

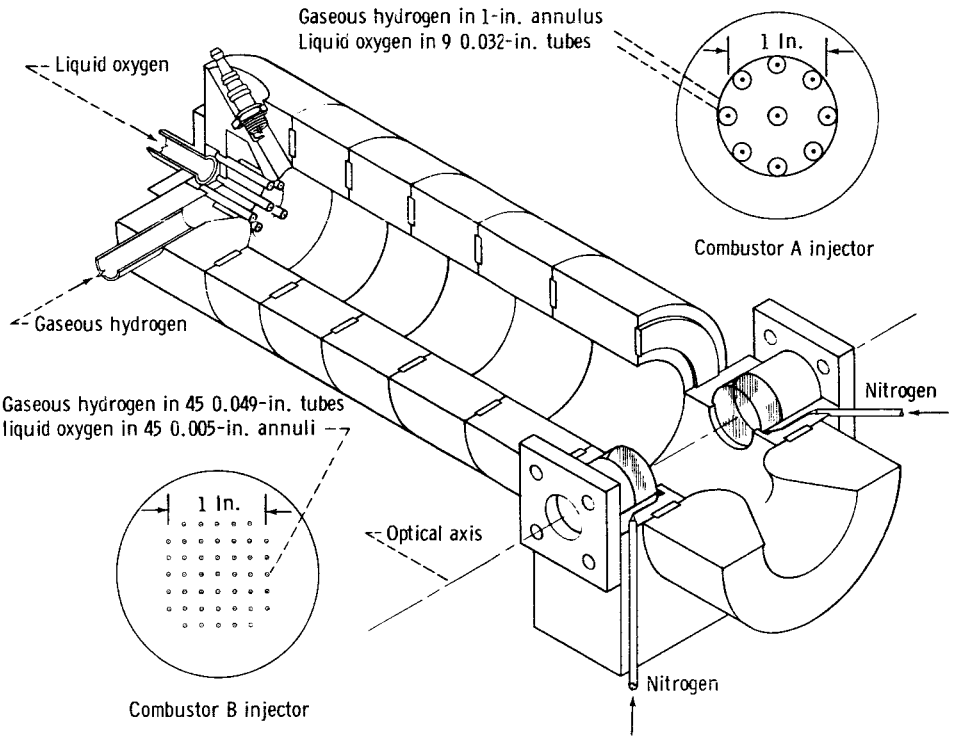

Fig. 1. - Gaseous-hydrogen - liquid-oxygen combustor. Distance from injector to optical axis variable from 0.8 to 21 inches; chamber diameter, 2 inches; nozzle diameter, 0.60 inch. Injector A, nine 0.032-inch liquid-oxygen jets parallel to low-velocity hydrogen flow. Injector B, 45 0.049-inch high-velocity hydrogen jets surrounded by 0.005-inch liquid-oxygen annuli.

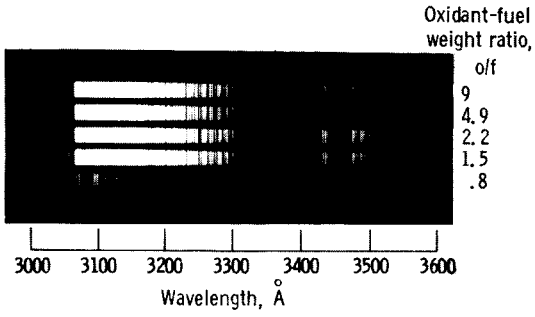

(a) Photographic spectrum of ultraviolet region; spectral slitwidth, 0.109 Å; Kodak type I-O film.

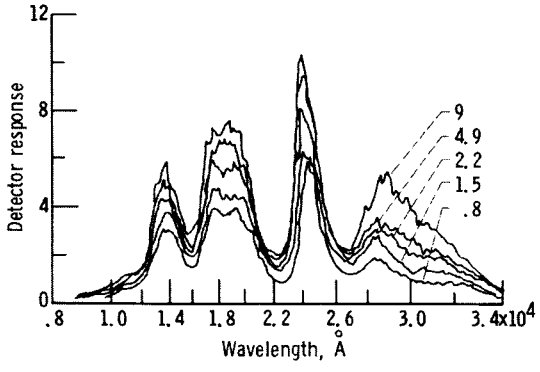

(b) Spectrogram of infrared region; indium antimonide detector; spectral slitwidth, 1000 Å; calcium fluoride and mirror optics.

Fig. 2. - Spectral radiation from combustor gases as function of wavelength.

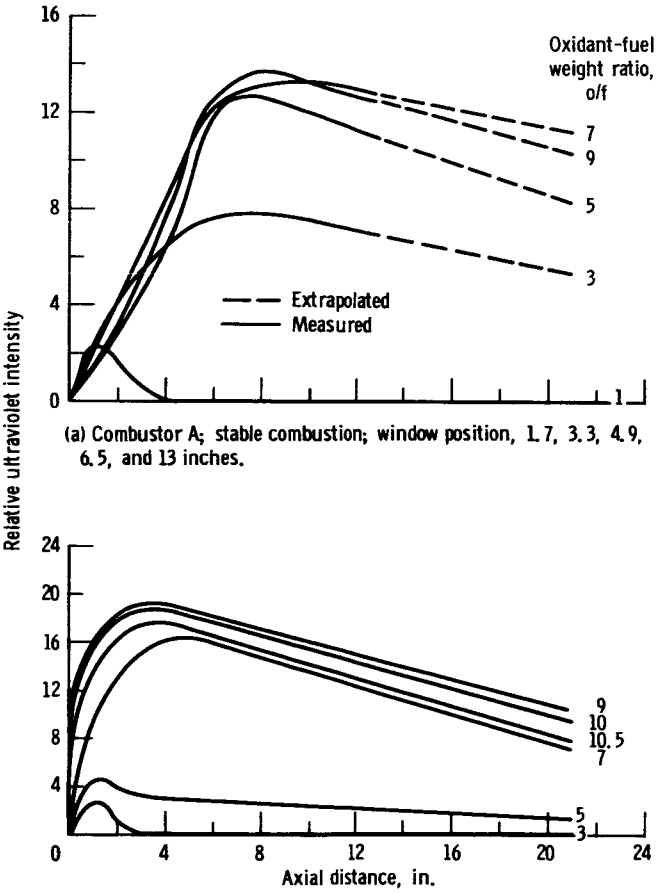

(a) Combustor A; stable combustion; window position, 1.7, 3.3, 4.9, 6.5, and 13 inches.

(b) Combustor B; unstable combustion; window position, 0.8, 4.0, 12.0, and 21 inches.

Fig. 3. - Relative ultraviolet intensities as function of axial distance from injector.

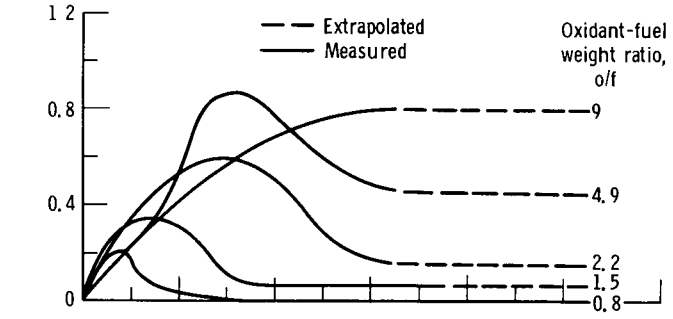

(a) Combustor A; stable combustion; window position, 1.7, 3.3, 4.9, 6.5, and 13 inches.

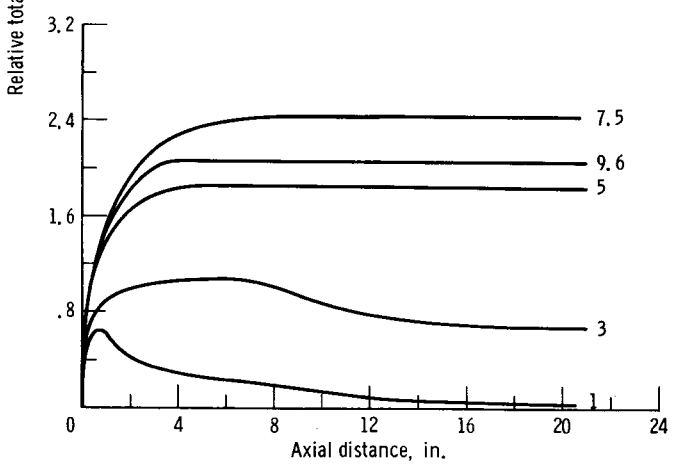

(b) Combustor B; unstable combustion; window position, 0.8, 4.0, 12.0, and 21 inches.

Fig. 4. - Relative total intensities as function of axial distance from injector.

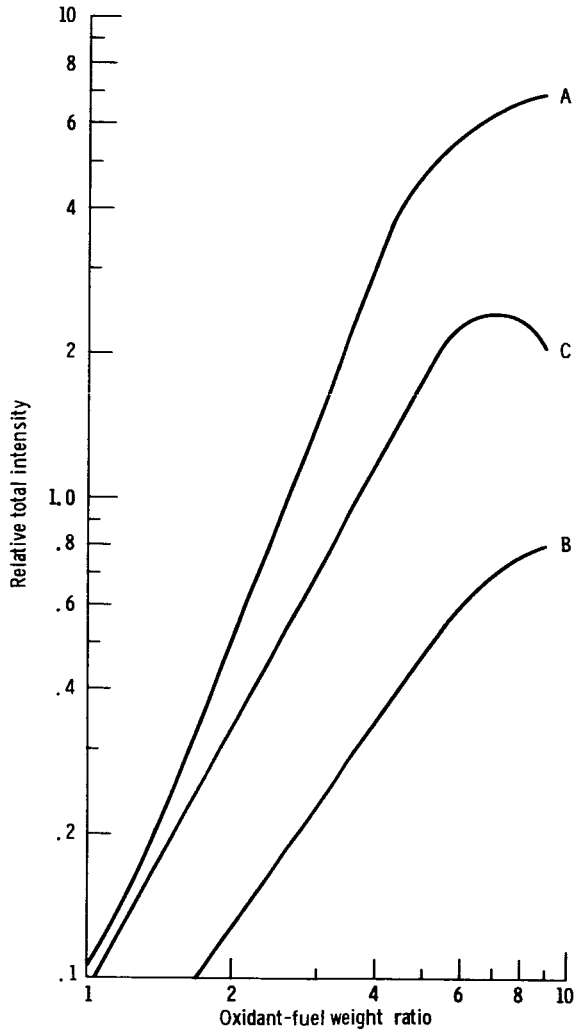

Fig. 5. - Relative total intensities as function of oxidant-fuel weight ratio. Curve A measured intensities of oxidized tungsten surface in combustor gas stream. Curve B measured intensities of gases 12-inches downstream in combustor A (from Fig. 4(a)). Curve C measured intensities of gases 12-inches downstream in combustor B (from Fig. 4(b)).

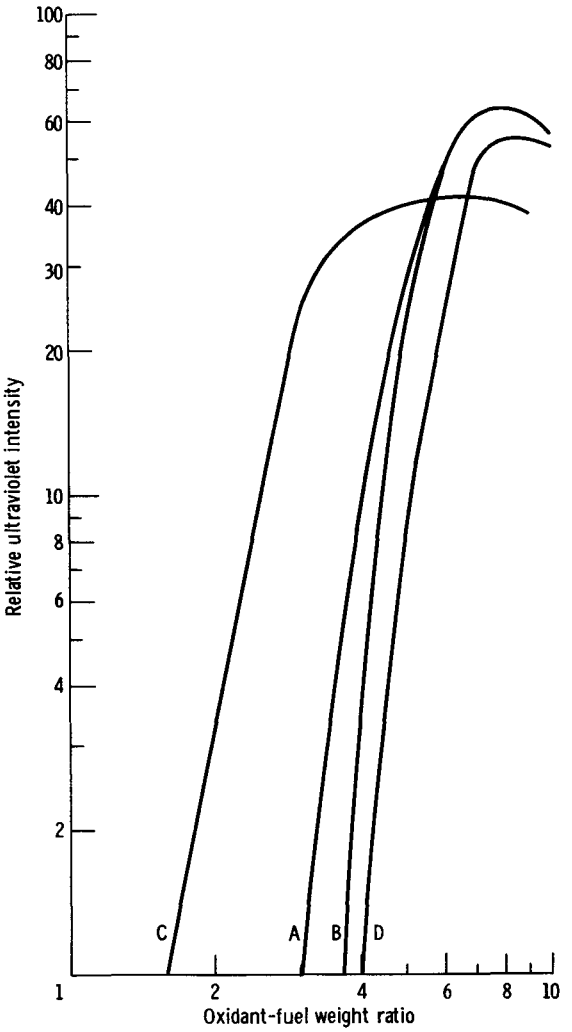

Fig. 6. - Relative ultraviolet intensities as function of oxidant-fuel weight ratio. Curve A calculated ultraviolet intensities at 3100 Å with emissivity of 1. Curve B calculated ultraviolet intensities at 3100 Å with emissivity related to OH concentration. Curve C corrected ultraviolet radiation 12-inches downstream in combustor A (from Fig. 3(a)). Curve D corrected ultraviolet radiation 12-inches downstream in combustor B (from Fig. 3(b)).

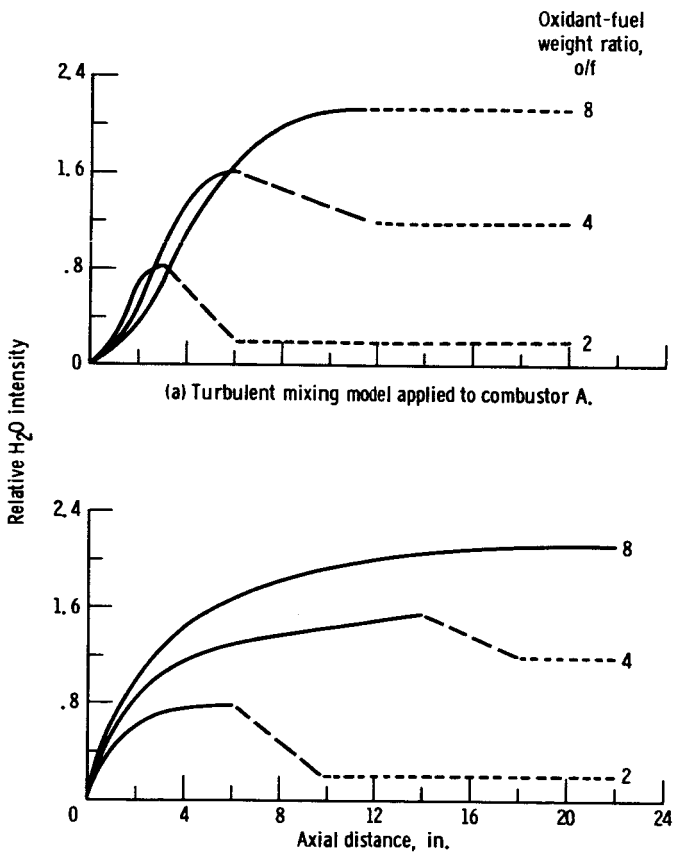

(a) Turbulent mixing model applied to combustor A.

(b) Vaporization model applied to combustor A.

Fig. 7. - Relative H_2O intensities at 24,000 Å as function of axial distance from injector. Zone 1, stoichiometric reaction; zone 2, mixing with excess H_2; zone 3, equilibrium products.

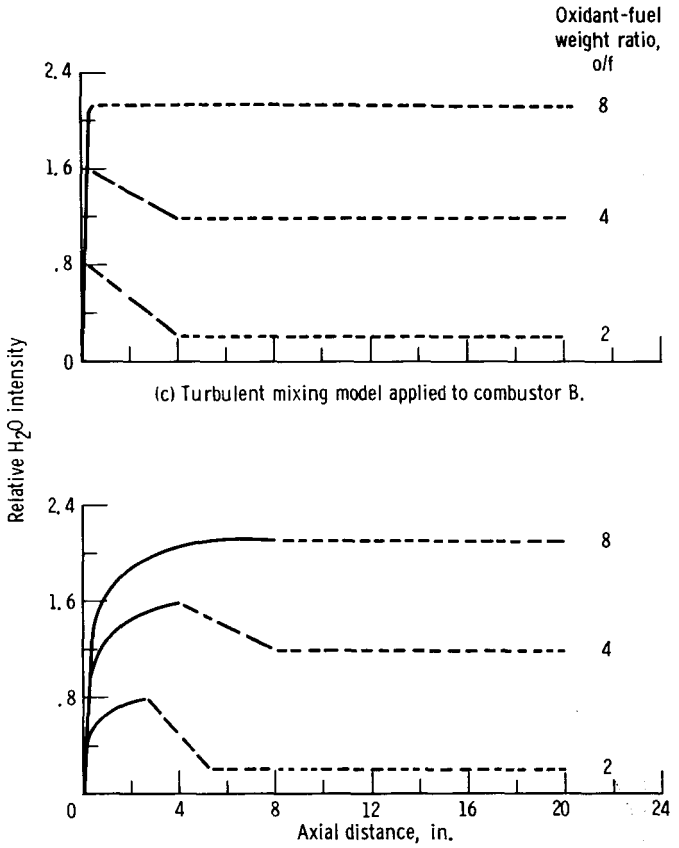

(c) Turbulent mixing model applied to combustor B.

(d) Vaporization model applied to combustor B.

Fig. 7. - Concluded. Relative H_2O intensities at 24,000 Å as function of axial distance from injector. Zone 1, stoichiometric reaction; zone 2, mixing with excess H_2; zone 3, equilibrium products.